PHYSICAL ORIGIN OF A MICROBURST SEEN BY RADAR PROFILER

David Atlas[1], Carlton W. Ulbrich[2], Christopher R. Williams[3]

[1]NASA Goddard Space Flight Center, Greenbelt, MD
[2]Dept. of Physics and Astronomy, Clemson University, Clemson, SC
[3]Univ. of Colorado & NOAA Aeronomy Laboratory, Boulder, CO

1. Introduction

During studies of the anatomy of an intense thunderstorm in the Rondonia region of the Amazon we were fortunate to observe a microburst passing directly over the Profiler radar (PR), thus making it possible to observe its characteristics in unprecedented detail. The burst occurred at the end of a period of intense rain resulting from melting of hail. The PR shows the antecedent microphysics and the downward acceleration of the air while the surface observations show the wind shift and gust front. The interpretation of these events is aided by a prior numerical simulation by Srivastava (1987). The origin of microbursts has also been treated by Proctor (1989), among others, and thoroughly reviewed by Wakimoto (2001). This is a case of a "wet" microburst; i.e. one that occurs with heavy precipitation as opposed to a "dry" one that occurs as a result of evaporation of light precipitation. Only this event and that reported by Wakimoto and Bringi (1988) have been observed with accompanying microphysical data.

2. Observations

The present study was based upon a major field campaign (Tropical Rain Measuring Mission – Large Scale Biosphere-Atmosphere Experiment – TRMM LBA) that took place in the Rondonia region of the Brazilian Amazon. The storm under discussion occurred on Feb 17, 1999 and has been discussed by Atlas and Williams [2003a, 2003b], (hereafter AW1 and AW2), and Williams and Rutledge (2003). Rickenbach et al. (2002) discuss the general environmental conditions and associated storm behavior.

2.1 Profiler Observations

The Profiler was located at Ji Parana (a map of the TRMM-LBA area is available at http://radarmet.atmos.colostate.edu/lba-trmm/instrumentation.html). Fig. 1 shows the PR profile of the Doppler spectra at 1726 (all times in UTC). The reflectivity spectral density (dBZ/(m s^{-1}) is shown by the color bar at the right. The white line corresponds to <V>, the mean Doppler velocity. The vertical profile of total reflectivity is shown to the left of the color bar. The 0°C level is at 5 km. There is no bright band at this time or on any of the profiles during the previous 15 min, and there was no linear depolarization ratio (LDR) on the S-POL polarimetric radar. This indicates the absence of snow. Instead the Z profile corresponds to that expected for melting hail (AW1). (S-POL was located at 42 km and 203° from the PR.)

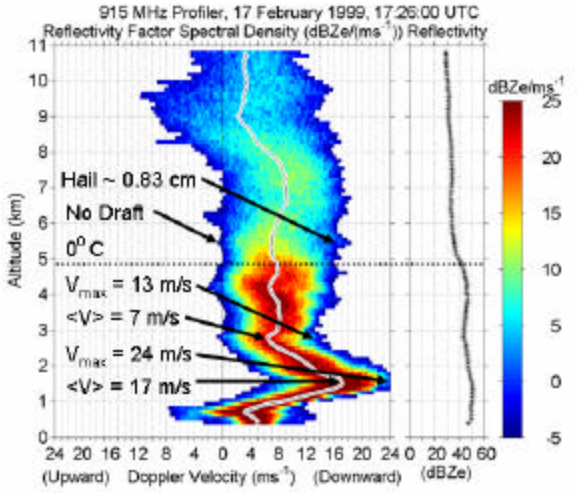

Fig.1: Profiler Doppler spectra (colorbar) and reflectivity versus height

The maximum downward velocity is 24 m s^{-1} at a height of 1.6 km. The acceleration begins at 2.8 km where the maximum downward velocity is 13 m s^{-1}. Assuming no change in the broadening of the spectrum due to turbulence between 2.8 and 1.6 km, the net increase is 11 m s^{-1}. Alternatively we may use the difference in <V> at the two levels: 7 and 17 m s^{-1}, respectively, or 10 m s^{-1}. The average speed of fall in this 1.2 km deep layer is 12 m s^{-1} thus taking 100 sec. The acceleration is then $(\Delta\langle V\rangle/\Delta t)\approx 0.1$ m s^{-2}. The

Corresponding author: Dr. David Atlas, Goddard Space Flight Center, Code 910, Greenbelt, MD,20771, E-mail: datlas@radar.gsfc.nasa.gov

divergence $\Delta V/\Delta h) \approx -0.08$ s^{-1}. (At time of writing we have been unable to find corresponding horizontal convergence; see below.)

In the five PR profiles between 1723:00 and 1725:00, there is evidence of weak updrafts of 1 to 3 m s^{-1} that vary with height between 2 and 5.5 km. These cause modulations of <V>. However, at 1725 there is no updraft below 3 km and <V>$\approx$ 8 m s^{-1} in the 2.2 to 2.8 km layer. Thus it appears that the above estimate of the acceleration is correct.

A horizontal map of the dual Doppler winds at 1 km height[1] (not shown) shows a clear minimum in the easterly winds at a position 6 km due south of the PR at 1720 UTC. However the convergence at this location is only about 10^{-3} s^{-1}. Since the storm is moving to the southwest and the Doppler observations occur 6 min after the microburst it is unlikely that the latter convergence center is associated with the microburst.

The lower bound of the Doppler spectra at the 0°C level during the period 1724 –1726 is zero, thus indicating the absence of any updraft there. The upper bound is 16 m s^{-1}. Assuming no spectral broadening due to other factors this corresponds to a maximum diameter of 0.83 cm based upon the fall speed law for hail due to Douglas (1964) and the correction to sea level due to Beard (1976). In order to correct for possible spectrum broadening we make the arbitrary assumption that the portion of the variance of the Doppler spectrum due to factors other than the fall speed spectrum is 0.5 of the total variance. Under this extreme assumption the upper bound of the fallspeed spectrum alone (say at 2 sigma) is 14.8 m s^{-1}. The latter value corresponds to a maximum hail diameter of 0.70 cm. Thus the probable range of hail diameters is between 0.70 and 0.83 cm. Such hail would melt completely in a fall of 5 km to the surface at a temperature of 28°C and relative humidity of 0.73 as observed in the sounding at Rebio Jaru (Rasmussen and Heymsfield, 1987). There was no hail observed in the vicinity of the Profiler. (Environmental conditions at the surface at Rebio Jaru: p=994 mb, T=28°C, RH=0.73, Wind=0.3 m/s at 240°)

[1]Provided by Andrea Williams, formerly of Dept of Atmospheric Sciences, Colorado State University.

A time-height record of Z, <V>, and Doppler spectrum width (SW) may be found in AW1. In the period 1710 to 1722, SW decreases from 4-5 m s^{-1} above 3 km to 2-4 m s^{-1} below that level. This is consistent with the melting of much of the hail near the 3 km level. However, values of 2-4 m s^{-1} are still greater than that attributable to rain alone even of rates of 100 mm h^{-1} (Atlas et al, 1973) or values computed for this storm from surface disdrometer data.

Fig. 1 also shows that the lower bound of the Doppler spectrum is considerably larger than zero in the altitude range from about 2.5 km down to about 1 km. Between 2.5 to 1.5 km the lower bound increases continuously and the entire Doppler spectrum is shifted to larger velocities. This clearly demonstrates that the vertical winds and the precipitation particles carried along by such winds are accelerating downward as discussed above.

2.2 Surface Data

Fig. 2 presents the surface observations at the PR for the entire hour starting at 1700. The initial temperature and RH are 30.4°C and 62%, respectively. The wind picks up with the onset of rain at 1704 but remains SE until 1722 when the effect of the microburst is manifested at the surface. It then shifts to N at 1728 and weakens until the gust of 15 m s^{-1} hits at 1732. Note the light winds after 1735 and the turning to the SSW after 1745. The peak gust of 15 m s^{-1} is in the lower range of bursts reported by Wakimoto (2001).

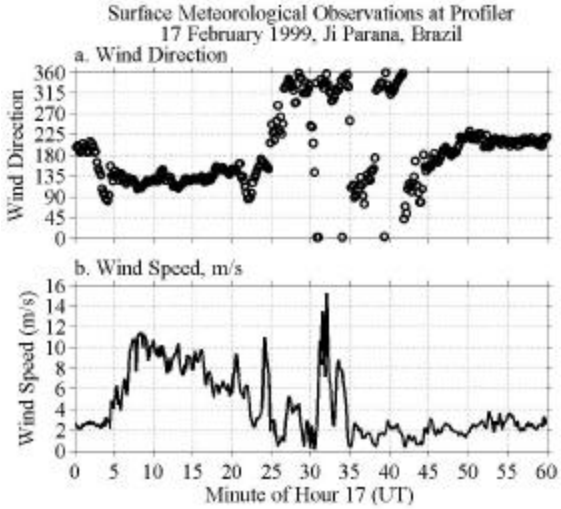

Fig. 2: Surface wind speed and direction

3. Comparison to theory

These and other features of the profiler records are in very good agreement with the numerical model of Srivastava (1987) (hereafter RS) for a downdraft driven by melting and evaporation of precipitation. He shows that the melting of ice proceeds slowly at first during its fall, due in part to precipitation loading and to sublimation, especially when the relative humidity (RH) is low (<0.50).

The initial conditions used by RS in his model are: pressure of 550 mb (height 5.1 km here) where the temperature is 0°C. These conditions are very similar to those for the present case. Fig. 3 shows the results of RS for the melting and evaporation of ice particles and water drops with an initial diameter of 0.7 cm. The latter diameter is close to that that deduced above from the PR. Each curve is marked by the RH. The sounding at Rebio Jaru for the time of the storm indicates that the RH in the altitude range 3 to 5 km (or in the 2 km below the assumed starting point) is roughly constant and 0.7.

The curves for RH=0.7 show that the mass of the liquid water drop is reduced very little by evaporation during its fall, whereas the mass of an ice particle decreases rapidly. The dashed line in Fig. 3 corresponds to a 50% reduction of ice mass. This decrease is 50% during a fall of about 2.2 km. The remaining 50% melts in a layer only 0.8 km thick. Hence the latent heat of melting is concentrated in a shallow layer near the height of final melt. Note that the higher the RH, the faster the ice particle melts. This difference is due to the increased release of latent heat at high RH due to the greater condensation of water vapor on the melting ice surface. Note that there is little effect with either altitude or RH on water drops. The fact that the latent heat extracted from the atmosphere is concentrated in a shallow layer indicates that this layer is more negatively buoyant than those above and causes the sharp increase in downdraft below.

The effects of these processes on the behavior of the downdraft have been calculated by RS using the initial environmental conditions specified above. He also assumes: a lapse rate of 7.0°C per kilometer; and an initial Marshall-Palmer ice size distribution with slope of 17 cm^{-1} and intercept of 0.08 cm^{-4}. The precipitation mixing ratio at the top of the downdraft is

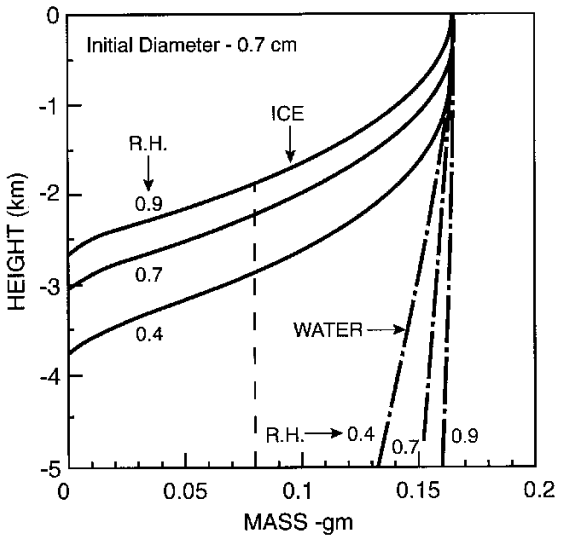

Fig. 3. Mass of an evaporating water drop and of ice in a melting ice particle falling in an atmosphere of the R.H. shown on each curve. Initial diameter of 0.7 cm. Lapse rate 7 °C km^{-1}. After Srivastava (1987).

assumed to be 3.9 g kg^{-1} and the reflectivity factor is taken to be 49 dBZ, in good accord with measurements by the disdrometer and the PR, respectively.

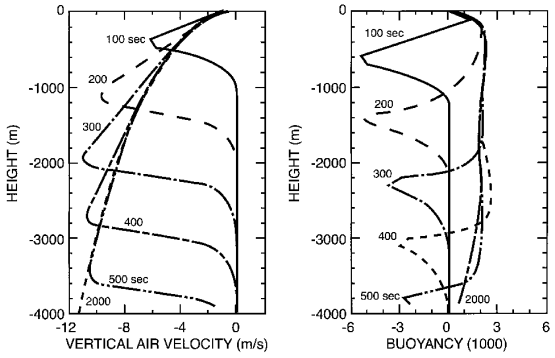

Fig. 4. a) Vertical velocity; b) Buoyancy.

Fig. 4a (left) shows the results of the calculations for the downdraft velocity as a function of height at 100 sec intervals; Fig. 4b shows the buoyancy at the same times [Buoyancy=$(T_d-T_e)/T_e$, where T_d and T_e are the virtual temperatures of the downdraft and environment, respectively]. It is seen that the peak downdraft descends and increases with time until it reaches a maximum value of about 11 m s^{-1} at 300 sec and at an altitude of 3 km below the starting point. This peak downdraft is

close to our estimate of 10 to 11 m s^{-1} downdraft deduced from Fig. 1. Note also that the negative buoyancy is concentrated in a layer just below the penetration depth of the draft.

4. Conclusions

The Profiler shows that the precipitation at and above the 0°C level is hail with maximum size of 0.7 to 0.83 cm. Most of the smaller hail would melt in about 2 km of fall from 5 km at the existing temperatures and humidity (70%). Doppler spectrum width decreases sharply at this level indicating melting to rain. The Profiler then shows the sudden increase in downdraft to a maximum of 10 to 11 m s^{-1} at the 1.6 km level. Surface winds show the rapid shift to northerly and a peak gust of 15 m s^{-1}, a relatively weak microburst. The numerical model of Srivastava (1987), with initial conditions close to those in the present storm, show the concentration of negative buoyancy near the bottom of the melting layer near 3 km and the peak downdraft of 10-11 m s^{-1}, in remarkable accord with observations.

Acknowledgement:

Drs. Atlas and Ulbrich are most appreciative of the support by NSF under Grant ATM 0223636, Atlas also acknowledges continued support under TRMM and the hospitality of NASA Goddard Space Flight Center. Dr. Williams' participation was supported in part by NASA Grant NAG5-9753 under the TRMM program.
We are deeply indebted to Prof. R. Srivastava of the University of Chicago for inspiring discussions without which this work could not have been done. We also thank Prof. Steven Rutledge and his colleagues at Colorado State University for data and insightful comments.

References:

Atlas, D., R. C. Srivastava , R. Sekhon, 1973: Doppler radar characteristics of precipitation at vertical incidence. *Rev. of Geophys. and Space Phys.* **11**, 1-35.

Atlas, D. and C.R. Williams, 2003a: The anatomy of a continental tropical convective storm. *J. Atmos. Sci.*, **60**, 3-15.

Atlas, D. and C.R. Williams, 2003b: Radar echoes from lightning and their microphysical environment. *Geophys. Res. Let,* **30**, 1262 (March 15, 2003).

Beard, K. V., 1976: Terminal velocity and shape of cloud and precipitation drops aloft. *J. Atmos. Sci.*, **33**, 851-864.

Douglas, R. H., 1964: Hail size distribution. *Proc. 11th Radar Wea. Conf.*, Amer. Meteor. Soc., Boston, 146-149.

Proctor, F.H., 1989: Numerical simulations of an isolated microburst. Part II: Sensitivity experiments. *J. Atmos. Sci*., **46**, 2143-2165.

Rasmussen, R.M. and A.J. Heymsfield, 1987: Melting and shedding of graupel and hail, Part II:Sensitivity study. *J. Atmos. Sci*., **44**, 2764-2782.

Rickenbach, T.M., R.N. Ferreira, J.B. Halverson, D.L. Herdies, and M.A. F. Silva Dias, 2002: Modulation of convection in the southwestern Amazon basin by extratropical stationary fronts. *J. Geophys. Res.,* **107** (D20), 8040, doi:10.1029/2000JD000263.

Srivastava, R., 1987: A model of intense downdrafts driven by the melting and evaporation of precipitation. *J. Atmos. Sci.*, **44**, 1752-1773.

Wakimoto, R.M. and V.N. Bringi, 1988: Dual-polarization observations of microbursts associated with intense convection: The 20 July storm during the MIST Project. *Mon. Wea. Rev.,* **116**, 1521-1539.

Wakimoto, R.M., 2001: Convectively driven high wind events. Chap. 7. *Severe Convective Storms* (Ed: C.W. Doswell III) Meteor. Mono, **28**, Chap. 7. 255-298.

Williams, A. G., and S. A. Rutledge, 2003: Kinematic, Microphysical and Latent Heating Aspects of Two MCSs Observed During TRMM-LBA. *Mon. Wea. Rev.,* submitted April, 2003.